

Optimization of Uniaxial Tensile Stress-Strain Response of 3D Angle Interlock Woven Fabric Composite using Weft Density and Draw-In Plan Variables

Muhammad Nasrun Faris Mohd Zulkifli, Mohamad Faizul Yahya*,
Suzaini Abdul Ghani
Textile Research Group, Faculty of Applied Sciences,
Universiti Teknologi Mara (UiTM), Shah Alam, MALAYSIA
*mfy@uitm.edu.my

Bilal Zahid
Department of Textile Engineering,
Faculty of Mechanical and Manufacturing Engineering,
NED University of Engineering and Technology, Karachi, PAKISTAN

ABSTRACT

Currently, 2D woven composites are extensively incorporated into a variety of technical automotive body parts and protective body armor owing to their excellent fabric strength performance. However, there is still a lack of attempts to utilize 3D woven fabrics for the same technical application. Hence, it is vital to examine the fundamental tensile strength of woven fabric composite materials when determining their suitability for end-use applications. This study aimed to investigate the novel effects of two parameters on the uniaxial tensile strength of a high-tenacity polyester three-layer 3D angle interlock (3DAI) woven fabric composite, namely, weave drafting draw-in insertion and weft density. Four different drafting patterns were considered: pointed (DRW 1), broken (DRW 2), broken mirror (DRW 3), and straight (DRW 4), for weft density at 14 and 25 pick.cm⁻¹. Samples of the 3DAI woven fabric reinforced with epoxy composite at different drafting patterns and weft density combinations were produced and tested. Consequently, the maximum tensile stress and strain were recorded in the woven fabric composite sample with DRW 4 and 25 pick.cm⁻¹ at 113 MPa and 11%, respectively. The study shows

that different weft densities and draw-in plan settings play a significant role in the tensile strength performance of the 3DAI woven composite.

Keywords: *3D Angle Interlock; Woven Composite; Uniaxial Tensile; Draw-In Plan; Weave Density*

Introduction

Previously, conventional 2D woven fabrics were extensively utilized as the main material for textile composites in technical applications. In addition, 2D woven composites have been used to replace metal and ceramic materials in automotive parts, especially because of their light weight, durability, and low manufacturing costs. Nevertheless, further studies have shown that 2D woven fabrics have weak delaminating resistance. This causes the ply fabrics inside the composite to split during matrix cracking upon force application, leading to out-of-plane properties in textile composites [1]-[4]. To resolve the interlaminar failure caused by 2D woven composites, scientists have developed a solution by introducing a three-dimensional (3D) woven fabric. The preference for 3D woven fabric in the composite is due to its better delamination resistance, good impact and ballistic resistance, and high in-plane properties. These mechanical properties are important for optimizing the technical applications of 3D woven fabrics. In general, knowledge of 3D woven fabric parameters and their impact on strength performance will promote the adoption of woven fabric composites in various technical applications. The existing literature shows a potential research gap regarding the drafting draw-in and weft density effects on 3DAI woven fabric performance. Thus, this paper aimed to investigate the uniaxial tensile stress-strain variation of a 3DAI woven fabric composite with different draw-in patterns and weft density combinations.

Literature Review

Recently, application of the 3D woven fabric to manufacture automotive body part has been receiving many interests from researchers. For an instance, study on 3D orthogonal fabric for the possibility of leaf spring application suggested that 3D fabric able to provide better tensile and flexural strength than 2D fabric [5]. Finite element simulation work on 3D woven composite on shock tower and fender applications able to achieve 25% and 30% lighter weight property respectively while successfully optimize the strength factor of the model [6], [7]. Analysis of different 3D weave structure for intend interior automobile application indicated that through thickness weave able to provide higher tensile strength performance than layer to layer weave [8]. Those studies

shows that determination and optimization the tensile breaking strength of the woven composite structure before its use is vital to ensure that the durability to withstand high amount of stress-strain load and elastic modulus can be meet.

Investigation of the tensile strength of 3D woven fabrics is vital, as it will help researchers to evaluate the fundamental hardness and ductility properties of woven composites before they can be recommended for suitable end-use applications. The tensile strength performance could be optimized by determining the woven fabric characteristics. Few studies have shown that the tensile strength of woven textile fabric depends on the fabric weft density and weave structure [8]-[11]. The weft density is the number of weft yarn insertions per fabric length; a high weft density indicates tightly packed weft yarns. Previous studies on the effects of weft density on single weave structures, such as 3D angle interlock [11], 2D plain [12] and 2D twill [13], found that a higher weft density produces a higher tensile strength owing to the increased yarn friction force at the weft horizon of the woven fabric. On the other hand, a study on a 2D plain weave by [9] reported an increase in weft density from 138 to 141 pick.10 cm⁻¹ had no effect on the tensile strength, as the increase in the weft density gap did not significantly elevate the yarn friction build-up. In addition to the weft density, different weave interlacement architectures affect the tensile strength of the woven fabric. The drafting approach played an important role in the resulting weave structure. During the weaving process, different drafting approaches involve varying the number of heald shafts used in drawing warp yarns [14]. Manipulation of the yarn-yarn interlacement sequence within the weave structure resulted in different woven fabric patterns. A comparative study on different types of weave structures showed that the 2D plain structure has the highest tensile strength compared to the twill and satin structures owing to a tighter interlacement pattern [15]. A compact weave structure contains tightly packed yarns, leading to friction force build-up and a higher tensile strength [16]-[17]. In contrast, a weave structure with a loose interlacement pattern allows for longer yarn elongation, leading to a lower tensile strength [18].

Research Method

Material preparation

The draw-in plan or drafting plan is a technique in which a certain number of heald frames are used during weaving manufacturing to produce the weave design, and the sequence order of the warp yarns (yarns from the vertical direction) is lifted or lowered by the heald frames. Four different draw-in plans were considered for the samples, which are pointed (DRW 1), broken (DRW 2), broken mirror (DRW 3), and straight (DRW 4) as depicted in Figure 1. For each draw-in plan, weft densities of 14 and 25 pick.cm⁻¹ were manufactured. The amount of weft density represents the total amount of weft yarns (yarns

inserted in the horizontal direction) per centimetre. All samples of the three-layer 3D angle interlock woven fabric were manufactured using the Sulzer rapier loom at 50 revolutions per minute (rpm), located at the Textile Weaving Workshop, UiTM Shah Alam, Malaysia. Throughout the weaving process, the weft density was automatically controlled by the system according to the warp density rate, which was set constant at 16 end.cm^{-1} . For all samples, the warp (90° , vertical) and weft (0° , horizontal) directions were constructed using spun and ply multifilament polyester yarns, respectively. Once completed, using the hand lay-up technique, a 3.7:1.7 mixture ratio of epoxy resin (BJC-39) and hardener was poured and spread evenly onto each sample in a mold plate, resulting in a polymer composite reinforced with 3D angle interlock woven fabric. The samples were left for 24 hours to ensure proper curing.

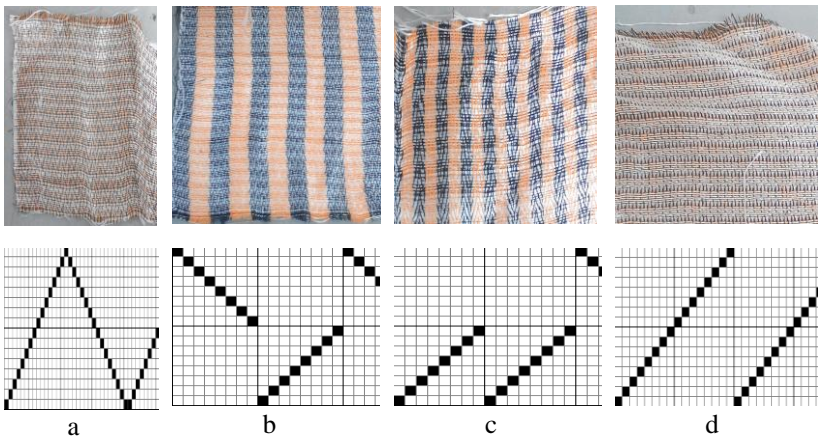


Figure 1: 3D angle interlock woven fabric samples based on the four draw-in plans; a) pointed (DRW 1), b) broken (DRW 2), (c) broken mirror (DRW 3), and d) straight (DRW 4)

Additionally, Figure 2 illustrates the 3D cross-sectional model of three-layer 3DAI woven fabric developed by using TexGen software. The model represents the actual yarn-yarn interlacing sequence order of the 3DAI used in this study.

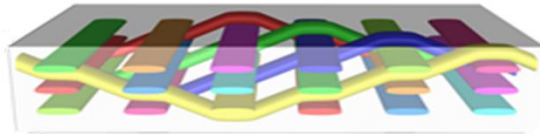


Figure 2: 3D illustration of three-layer 3DAI woven fabric

Yarn strength analysis

Yarn samples were prepared with 250 mm sample length. Yarn strength analysis was experimented on Tenso Lab 5000 strength tester machine. All yarn specimens were subjected to tenacity test based on the ASTM D2256, using a 5 kN load cell with the speed constant at 500 mm/min and the yarn pretension was set at 0.1 N. Yarn tenacity were calculated as the maximum amount of force at break of the yarn divided with the yarn linear density in Tex. Five readings were recorded to calculate the average result of yarn tenacity performance.

Crimp analysis

The fabric crimp samples were prepared with 200 mm length accordingly to the warp and weft directions based on ASTM D3883. A single yarn was carefully pulled out from the woven fabric specimen and ten readings were recorded to ensure consistency. In Equation 1, the crimp presence, C , can be measured by identifying the length of yarn within the woven fabric, L_f and the length of yarn pulled out and straighten from the woven fabric, L_y . The analysis was repeated five times to calculate the average result.

$$C = \frac{L_y - L_f}{L_f} \times 100\% \quad (1)$$

Woven composite tensile strength

The prepared samples were cut into specimens with 200 mm length, 25 mm width, and 1 mm thickness. The uniaxial tensile strength evaluation was conducted on Tenso Lab 5000 strength tester machine. All samples were subjected to tensile tests based on the ASTM D3039 standard, using a 50 kN load cell with a crosshead speed set constant at 100 mm/min. For each combination of draw-in plan and weft density, five samples were prepared and tested to measure the average breaking strengths in the weft and warp directions, respectively.

Result and Discussion

Yarn properties

Table 1 presents the details of spun and plied filament polyester yarns used in this research work. Identification of physical property shows that plied filament yarn provided with high value of yarn linear density compared to both spun yarns. In addition, plied filament yarn outperformed yarn tenacity strength performance by 1036.9 cN/Tex higher than both black and orange spun yarns at 105.9 and 331.4 cN/Tex. Configuration of ply technique between two sets of filament yarn shows a good outcome to improve the yarn strength.

Table 1: Yarn properties used to manufacture 3D angle interlock woven composite

Type of yarn structure	Mass of yarn (g)	Yarn linear density (Tex)	Yarn tenacity (cN/Tex)
Spun polyester black	8	26	105.9
Spun polyester orange	9	30	331.4
Plied filament polyester	1.5	100	1036.9

Crimp properties

Table 2 shows the readings of yarn crimp presence on warp and weft direction of the woven fabric respectively based on the variations of draw-in plan (DRW). It can be seen from the Table 2 that 14 pick.cm⁻¹ and 25 pick.cm⁻¹ on DRW 1 and 4 resulted highest crimp presence in warp direction with 7.8%, and 9.5%, respectively. Meanwhile, 14 pick.cm⁻¹ and 25 pick.cm⁻¹ on DRW 2 and 3 at weft direction consistently presented the lowest crimp with 3.1 and 4.3%, respectively.

Table 2: Crimp presence (%) in warp and weft directions of 3DAI woven fabric sample

Direct. Sample	Crimp in warp direction (%)				Crimp in weft direction (%)			
	DRW1	DRW2	DRW3	DRW4	DRW1	DRW2	DRW3	DRW 4
14	7.7	7.1	7.1	7.8	3.6	3.1	3.1	3.7
25	9.5	9.1	9.1	9.5	4.7	4.3	4.3	4.8

This finding were consistent with several studies [19]-[20] reported on crimp. The observation on this 3DAI woven fabric shows that warp direction fabric produced high crimp percentage as it exhibited more yarn interlacement sequence than weft counterpart. Meanwhile, changes of different draw-in plan factor indicate an interesting pattern where DRW 1 and 4 produced higher percentage of crimp than DRW 2 and 3.

Uniaxial tensile response on weft density of 14 pick.cm⁻¹

Figure 3 shows the tensile stress-strain of 3DAI woven composite based on 14 pick.cm⁻¹. According to the curve line behaviour, the composite stress-strain curve line was reacted as elastic behavior which majorly affected by the woven fabric. Hence the graph was divided into 3 phases to represents the behavior of composite [18]-[19]. In the first phase, the stress-strain curve pattern of DRW 1 and 2 is shown to be above on top of DRW 3 and 4 by % strain at the first tensile load. Within phase 1, however, the stress-strain value of the DRW 1 curve line had abruptly altered from 0.4% to 0.6% strain. In the second phase,

all of the work's draw-in plans demonstrated a close curve pattern in strain ranges of 0.6% to 1.2%. The curve of all draw-in plans demonstrated significant stress-strain fluctuation between 1.2% and 1.6% strains in the third phase. It's worth noting that the DRW 4 curve behaviour has the highest stress and strain results, with 31.77 MPa and 1.6%, respectively. DRW 2, on the other hand, had the lowest stress value of 21.00 MPa and the smallest strain of 1.4%.

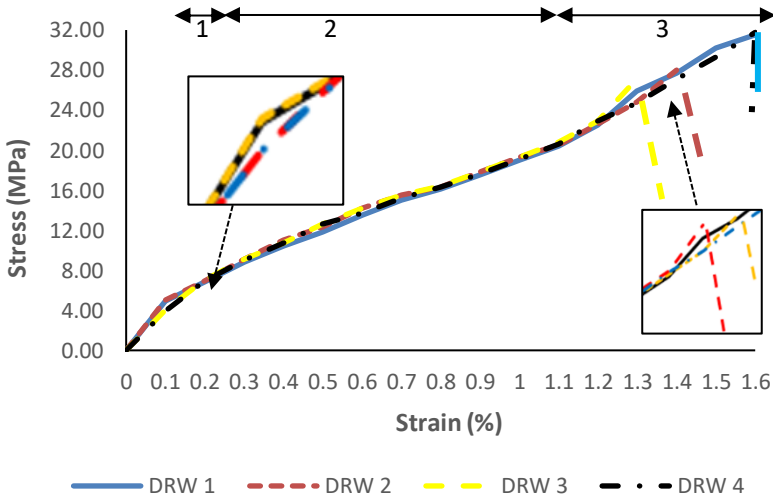


Figure 3: Stress-strain curves in the warp direction, for all draw-in plans with 14 pick.cm⁻¹ density

The stress-strain curve behaviour of 14 pick.cm⁻¹ of 3D woven composite in the weft direction is shown in Figure 4. The curve line was divided into two distinct phases in general. Phase 1, DRW 1 and 4, produced the highest stress-strain curve line in the 0 to 2.5 % strain region. Within the 2.5% strain range, however, DRW 2 and 3 had the lowest stress-strain curve. All draw-in plans in the second phase revealed a stress-strain fluctuation curve line in 4% to 5% strain ranges. At 6 % strain, the DRW 1 and 4 curve lines appeared on top of the DRW 2 and 3 curve lines. In general, DRW 4 has the greatest stress value of 64 MPa and accordingly % strain.

Uniaxial tensile response on weft density of 25 pick.cm⁻¹

Figures 5 and 6 show the stress-strain variations in the warp and weft directions, respectively, for the four draw-in plans with 25 pick.cm⁻¹. Compared to the 14 pick.cm⁻¹ cases, the stress-strain curves in the warp direction for the 25 pick.cm⁻¹ indicated three distinct phases. In the first phase, all curves followed a linear trend with similar values. The second phase was in between 0.6% to 2.7% strain. In the initial part of the second phase, between

0.6% and 1.7%, DRW 3 had the lowest stress value, while DRW 1 and DRW 4 had the highest values. At the start of the third phase, DRW 1 had the lowest value. However, the trend was reversed with DRW 1 recording the highest stress after 3.7% strain. Marked deviations between the curves were then observed between 3.7% and 4.5% strain. Eventually, the curves for DRW 1 and DRW 4 ended at a strain of 4.6%, whereas DRW 2 and DRW 3 ended at 4.5%. The highest and lowest maximum stresses were 48 MPa and 46 MPa, for DRW 1 and DRW 3, respectively.

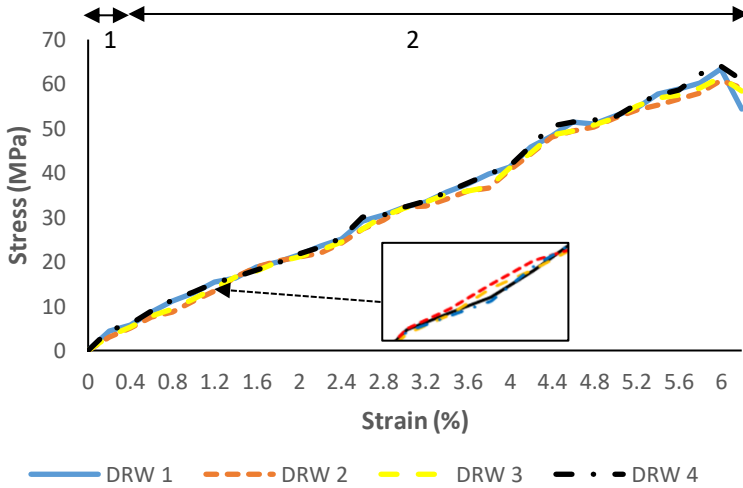


Figure 4: Stress-strain curves in the weft direction, for all draw-in plans with 14 pick.cm⁻¹ density

The three distinct phases of the stress-strain curves were also present in the weft direction, as shown in Figure 6. Similarly, close trends of all curves in the first stage were observed until 0.7% strain. Similar profiles were seen for DRW 1 and DRW 4, indicating markedly higher stress values than DRW 2 and DRW 3 in the second phase. At 5.5%, there was a noticeable rise in DRW 2 to yield the highest stress value at this point, and this trend continued until DRW 2 reached the failure point at around 9% strain. Eventually, DRW 4 reached its failure point at a strain of 11%, with the highest maximum stress of 113 MPa. The lowest maximum stress was for DRW 2, at 108 MPa and 9% strain.

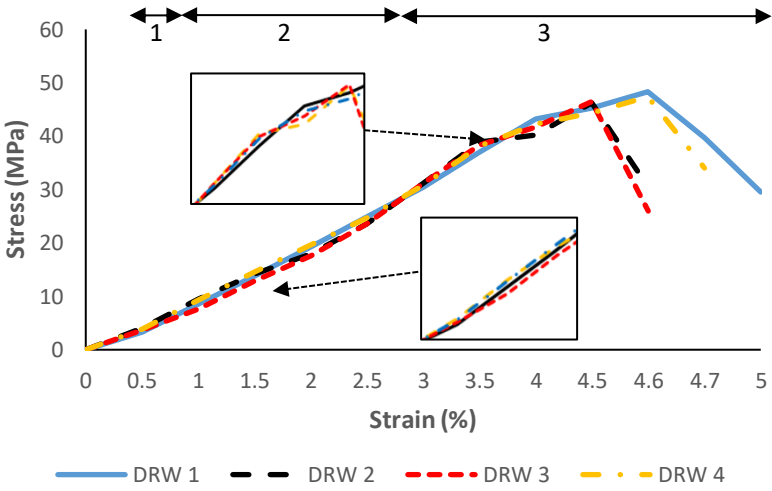


Figure 5: Stress-strain curves in the warp direction, for all draw-in plans with 25 pick.cm⁻¹ density

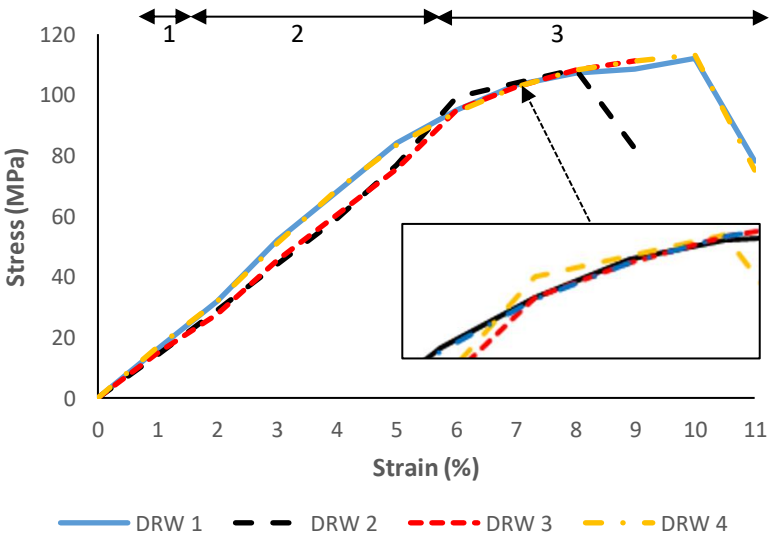


Figure 6: Stress-strain curves in the weft direction, for all draw-in plans with 25 pick.cm⁻¹ density

Uniaxial tensile stress-strain response discussion

In general, it can be seen that weft densities of 14 and 25 pick.cm⁻¹ in the warp direction samples in Figures 3 and 4 produced a nearly straight or linear line look alike pattern compared to the other counterparts in the weft direction, as shown in Figures 4 and 6. This condition shows that the uniaxial tensile stress-strain behaviour of was still significantly affected by the epoxy resin. Meanwhile, the woven composite sample in the weft direction tends to generate a nonlinear pattern. The presence of more weft yarn directly impacts yarn-yarn interlacement, thus resulting in a high requirement build-up [21]-[24]. Hence, the uniaxial tensile stress-strain of high weft density in the weft direction begins to react according to the nature of the nonlinear woven fabric tensile stress-strain performance. The close trends of the stress-strain curves for all draw-in plans in the 14 pick.cm⁻¹ samples indicate that the stress resistance build-ups were almost uniform, particularly for the first and second phases. In the first phase, when the tensile loads were low, all draw-in plans exhibited similar behavior. The fluctuation of the curved lines within the third phase of 14 pick.cm⁻¹ of the warp sample suggested an uneven stress performance of the loaded warp yarn. It can be seen that, DRW 1 and 4 gave the highest maximum stress before break value. This is because both DRW 1 and 4 recorded the least stress value reduction on the loaded yarn during composite elongation compared to the other counterparts, DRW 2 and DRW 3. The elongation rate of deformation is dependent on the stress performance of the loaded warp yarn. A greater length of warp yarn floating on woven fabric will produce a high amount of loaded warp yarn stress strength. The increasing tensile strengthening induced slightly higher resistance build-ups in the warp direction for all the plans in the second phase. The discrepancies in the resistance build-ups were significant in the third phase, with DRW 1 and DRW 4 indicating the least strength loss after tensile straightening.

On the other hand, 14 and 25 pick.cm⁻¹ in the weft direction in Figures 4 and 6 have a tendency to generate a nonlinear or straight curve line. The inconsistency of uniaxial tensile stress-strain behavior between low and high amounts of weft density is highly due to the woven fabric interlacement-resistant break capability within the composite matrix [22], [25]. The presence of more yarn-yarn interlacement sequences owing to the high weft density will create a more interlacement sequence. As a result, a large amount of load-breaking resistance is produced. Evidently, in the latter, there were higher stress build-ups in the weft direction for DRW 1 and DRW 4, as shown by the larger discrepancies between DRW 2 and DRW 3. This finding agrees with those of the studies reported in [14], [19]. For all draw-in plans, the tensile straightening in the weft direction induced inconsistent stress, which resulted in fluctuations in the maximum stress, leading to the failure point. This inconsistent behavior can be attributed to the different yarn interlacement amounts in each draw-in plan. Thus, the lowest interlacement and crimp

percentages in DRW 1 and DRW 4 resulted in the highest maximum stresses at failure.

Conclusion

In this study, the novel effects of weave draw-in plans and weft density on the tensile strength performance of 3DAI woven composites were investigated. Samples comprising various combinations of the four draw-in plans and four weft densities were tested. It can be noticed that the DRW 4 draw-in plan with 25 pick.cm⁻¹ weft density resulted in the highest maximum stress and strain at 113 MPa and 11%, respectively. Interestingly, the DRW 1 plan was found to exhibit a similar stress-strain profile similar to that of the other plans at lower loads. As the load increased, higher stress values were recorded for DRW 1. It is concluded that the stress-strain performance of the 3DAI woven composite varies with the draw-in plan and weft density. A high weft density positively influences the tensile strength. Meanwhile, each DRW plan showed that different settings produced a distinctive tensile performance.

Contributions of Authors

The authors confirm the equal contribution in each part of this work. All authors reviewed and approved the final version of this work.

Funding

This work was supported by through research grant 600-IRMI 5/3/LESTARI (044/2019).

Conflict of Interests

All authors declare that they have no conflicts of interest.

Acknowledgment

The authors would like to thank Faculty of Applied Sciences, Universiti Teknologi MARA (UiTM) Shah Alam for the facilities support, Universiti Teknologi MARA (UiTM) for the internal funding.

References

- [1] B. Kumar and J. Hu, "Woven fabric structures and properties," *Engineering of High-Performance Textiles, The Textile Institute Book Series*, pp. 133–151, 2017, doi: 10.1016/B978-0-08-101273-4.00004-4.
- [2] Mohamed Nasr Saleh, Ying Wang, Arief Yudhanto, Adam Joesbury, Prasad Potluri, Gilles Lubineau and Constantinos Soutis, "Investigating the Potential of Using Off-Axis 3D Woven Composites in Composite Joints' Applications," *Applied Composite Materials*, vol. 24, no. 2, pp. 377–396, 2017, doi: 10.1007/s10443-016-9529-9.
- [3] B. Kazemianfar, M. Esmaceli, and M. R. Nami, "Response of 3D woven composites under low velocity impact with different impactor geometries," *Aerospace Science and Technology*, vol. 102, pp. 105849, 2020, doi: 10.1016/j.ast.2020.105849.
- [4] T. Gereke and C. Cherif, "A review of numerical models for 3D woven composite reinforcements," *Composite Structures*, vol. 209, no. October, pp. 60–66, 2019, doi: 10.1016/j.compstruct.2018.10.085.
- [5] V. Khatkar, B. K. Behera, and R. N. Manjunath, "Textile structural composites for automotive leaf spring application," *Composites Part B: Engineering*, vol. 182, no. November 2019, pp. 107662, 2020, doi: 10.1016/j.compositesb.2019.107662.
- [6] W. Tao, P. Zhu, Z. Liu, and W. Chen, "Lightweight design of three-dimensional woven composite automobile shock tower," *Proceeding. Conference: ASME 2018 International Design Engineering Technical Conferences*, vol. 3, pp. 1–10, 2018, doi: 10.1115/DETC2018-85519.
- [7] W. Tao, Z. Liu, P. Zhu, C. Zhu, and W. Chen, "Multi-scale design of three dimensional woven composite automobile fender using modified particle swarm optimization algorithm," *Composite Structures*, vol. 181, pp. 73–83, 2017, doi: 10.1016/j.compstruct.2017.08.065.
- [8] M. Kashif, S. T. A. Hamdani, Y. Nawab, M. A. Asghar, M. Umair, and K. Shaker, "Optimization of 3D woven preform for improved mechanical performance," *Journal of Industrial Textiles*, vol. 48, no. 7, pp. 1206–1227, 2019, doi: 10.1177/1528083718760802.
- [9] J. S. Lim, B. H. Lee, C. B. Lee, and I.-S. Han, "Effect of the Weaving Density of Aramid Fabrics on Their Resistance to Ballistic Impacts," *Engineering*, vol. 04, no. 12, pp. 944–949, 2012, doi: 10.4236/eng.2012.412a119.
- [10] M. Dahale et al., "Effect of weave parameters on the mechanical properties of 3D woven glass composites," *Composite Structures*, vol. 223, no. March, pp. 110947, 2019, doi: 10.1016/j.compstruct.2019.110947.
- [11] F. M. Z. Nasrun, M. F. Yahya, S. A. Ghani, and M. R. Ahmad, "Effect of weft density and yarn crimps towards tensile strength of 3D angle interlock woven fabric," *AIP Conference Proceedings*, vol. 1774, pp. 1-7,

- 2016, doi: 10.1063/1.4965051.
- [12] H. Özdemir and E. Mert, "The effects of fabric structural parameters on the breaking, bursting and impact strengths of diced woven fabrics," *Tekst. ve Konfeksiyon*, vol. 23, no. 2, pp. 113–123, 2013.
- [13] O. G. Ertaş, B. Zervent Ünal, and N. Çelik, "Analyzing the effect of the elastane-containing dual-core weft yarn density on the denim fabric performance properties," *The Journal of The Textile Institute*, vol. 107, no. 1, pp. 116–126, 2016, doi: 10.1080/00405000.2015.1016319.
- [14] M. Ashir, D. M. P. Vo, A. Nocke, and C. Cherif, "Adaptive fiber-reinforced plastics based on open reed weaving functionalization," *IOP Conference Series: Materials Science and Engineering*, vol. 406, no. 1, pp. 1-9, 2018, doi: 10.1088/1757-899X/406/1/012063.
- [15] G. A. Nassif, "Effect of weave structure and weft density on the physical and mechanical properties of micro polyester woven fabrics," *Journal of American Science*, vol. 9, no. 3, pp. 1326–1331, 2012.
- [16] S. Dai, P. R. Cunningham, S. Marshall, and C. Silva, "Influence of fibre architecture on the tensile, compressive and flexural behaviour of 3D woven composites," *Composites Part A: Applied Science and Manufacturing*, vol. 69, pp. 195–207, 2015, doi: 10.1016/j.compositesa.2014.11.012.
- [17] J. S. Jones, R. R. Rowles, K. N. Segal, and D. L. Polis, "Comparative study of 3-dimensional woven joint architectures for composite spacecraft structures," *International SAMPE Technical Conference*, pp. 1-18, 2011.
- [18] J. Hu, *Structure and Mechanics of Woven Fabric*. Woodhead Publishing, 2004.
- [19] C. Huang, L. Cui, H. Xia, and Y. Qiu, "Influence of Crimp and Inter-Yarn Friction on the Mechanical Properties of Woven Fabric under Uniaxial / Biaxial Tensile Loading," *Fibres and Textiles In Eastern Europe*, vol. 6, no. 144, pp. 43–52, 2020, doi: 10.5604/01.3001.0014.3797.
- [20] S. Ö. Hacıoğulları and O. Babaarslan, "An investigation on the properties of polyester textured yarns produced with different fiber cross-sectional shapes," *Industria Textila*, vol. 69, no. 4, pp. 270–276, 2018, doi: 10.35530/it.069.04.1281.
- [21] H. Zhou, X. Xiao, K. Qian, and Q. Ma, "Numerical simulation and experimental study of the bursting performance of triaxial woven fabric and its reinforced rubber composites," *Textile Research Journal*, vol. 90, no. 5–6, pp. 561–571, 2020, doi: 10.1177/0040517519871943.
- [22] H. Özdemir and B. M. İçten, "The mechanical performance of plain and plain derivative woven fabrics reinforced composites: tensile and impact properties," *The Journal of The Textile Institute*, vol. 109, no. 1, pp. 133-145, 2018, doi: 10.1080/00405000.2017.1333719.
- [23] H.A. Aisyah, M.T. Paridah, A. Khalina, S.M. Sapuan, M.S. Wahab, O.B. Berkalp, C.H. Lee and S.H. Lee, "Effects of fabric counts and weave designs on the properties of Laminated Woven Kenaf/Carbon fibre

- reinforced epoxy hybrid composites,” *Polymers*, vol. 10, no. 12, pp. 1-19, 2018, doi: 10.3390/polym10121320.
- [24] M. N. F. M. Zulkifli and M. F. Yahya, “3D angle interlock woven fabric mechanical tensile strength based on various fabric weft densities,” *Journal of Mechanical Engineering*, vol. 5, no. Specialissue 1, pp. 92–103, 2018.
- [25] M. Li, P. Wang, F. Boussu, and D. Soulat, “Investigation of the Strength Loss of HMWPE Yarns During Manufacturing Process of 3D Warp Interlock Fabrics,” *Applied Composite Materials*, vol. 29, no. 0123456789, pp. 1-15, 2021, doi: 10.1007/s10443-021-09951-6.